Available online at www.sciencedirect.com

SCIENCE DIRECT®

International Journal of Psychophysiology 54 (2004) 201–220

INTERNATIONAL JOURNAL OF PSYCHOPHYSIOLOGY

www.elsevier.com/locate/ijpsycho

Recovering dipole sources from scalp-recorded event-related-potentials using component analysis: principal component analysis and independent component analysis

John E. Richards*

Department of Psychology, University of South Carolina, Columbia, SC 29208, United States

Received 23 October 2003; received in revised form 4 December 2003; accepted 18 March 2004

Abstract

Principal component analysis (PCA) and independent component analysis (ICA) were examined in their ability to recover dipole sources from simulated data. Datasets of EEG segments were generated that contained cortical sources that were temporally overlapping or non-overlapping, and dipole sources with varying degree of spatial orthogonality. For temporal overlapping sources, both PCA and ICA resulted in components that required multiple-source equivalent current dipole models. The spatially overlapping sources affected the PCA method more than ICA, resulting in single PCA components in which all non-orthogonal sources were represented. For both PCA and ICA, dipole models with fixed-location dipoles successfully accounted for most of the variance in the component weights, even when the spatial or temporal overlap of the generating sources required multiple-dipole models.

Keywords: Event-related-potential component; Principal component analysis (PCA); Independent component analysis (ICA)

1. Introduction

A common view of event-related-potential (ERP) components is that they are defined by scalp topography, temporal morphology, and relation to experimental variables (Donchin et al., 1978; Fabiani et al., 2000; Spencer et al., 1999). I suggest that this view of ERP components represents "cognitive psychophysiology", where the scalp topography or the temporal activity is sufficient to achieving the psychological goals of psychophysiology. "Cognitive neuroscience" would place two additional qualifications for ERP components. First, ERP components should be defined by specific systems in the brain where they are generated, and second, other neuroimaging tools (e.g., fMRI, PET) give complementary information regarding these components. The present

* Tel.: +1 803 777 2079; fax: +1 803 777 9558.
E-mail address: richards-john@sc.edu.

0167-8760/$ - see front matter © 2004 Elsevier B.V. All rights reserved.
doi:10.1016/j.ijpsycho.2004.03.009

study shows that component analysis methods, such as principal component analysis (PCA) and independent component analysis (ICA), may recover cortical and intracerebral sources of scalp-recorded ERP and that this technique aids in the goal of defining brain locations for ERP components.

The analysis of ERP components has been aided by PCA in two ways. First, temporal PCA has been useful in determining the time course of ERP activity. Temporal PCA uses as variables the ms intervals for which the EEG (ERP) has been sampled and uses as observations the EEG channels. The eigenvectors from this analysis are then plotted to represent uncorrelated sources of temporal activity in the ERP signal (Chapman and McCrary, 1995; Dien, 1998; Spencer et al., 1999). The sequence of eigenvector weights from this analysis may be used to infer peaks in the ERP, such as the P3 (at ~300 ms post-stimulus), N4, and so forth. Second, "spatial" PCA has been proposed as a method to recover the topographical aspects of ERP components (Dien, 1998; Richards, 2003; Spencer et al., 1999). Spatial PCA uses as variables the EEG channels and uses as observations the ms intervals for which the EEG (ERP) has been sampled. A recent application of PCA has combined spatial and temporal PCA to analyze the components found in the P3a and P3b for recognition memory (Spencer et al., 1999). Thus, the temporal and topographical aspects of ERP components may be studied with PCA.

Can PCA be used as an aid to the cognitive neuroscience goal of the identification of the brain areas in which the ERP components are generated? One way in which this might proceed is to identify a set of weights that represent the topographical information from the ERP (i.e., Spencer et al., 1999). These weights can then be used with dipole source analysis (e.g., Scherg, 1990, 1992; Scherg and Picton, 1991; Huizenga and Molenaar, 1994). Dipole source analysis hypothesizes a (a set of) dipole (s) located in the cortex representing a current source generated by a large number of neurons located in a discretely bounded area. The "forward solution" may be calculated that represents the electrical current that would occur on the scalp from a dipole with specified location and magnitude vectors. The forward solution current is compared with the component weights, and the dipole location/magnitude adjusted to achieve a best fit between the hypothesized current and the component weights. Dien (Dien, 1999; Dien et al., 1997) has studied psychosocial and cognitive processes with this method, and Richards (2003) has studied cortical sources of ERP in the prosaccade–antisaccade task with this method.

There are several characteristics of PCA that suggest it is suitable for examining cortical sources. The PCA technique is a linear decomposition of data that results in a set of weights, eigenvectors, that form the basis for a new coordinate system. The eigenvector weights describing one dimension are orthogonal to the dimensions described by other eigenvectors. If multichannel EEG recordings are processed by PCA using the channels as variables and the time points as observations, the resulting eigenvector matrix is a set of topographic scalp maps (Jung et al., 2000a). The component analysis of ERP scalp activity assumes that there are discrete sources of neural activity that sum linearly to form the observed electrical activity recorded with electrodes on the scalp (Makeig et al., 1996, 1997). The decomposition of the variance in the ERP signal with PCA assumes that this activity can be distinguished via its co-occurrence in the spatial coordinate system found with PCA. Thus, the eigenvector weights themselves could be used in equivalent current source analysis to model the dipoles that generated scalp-recorded EEG activity. It has been shown that the dipoles underlying the generation of scalp electrical activity may in some circumstances be recovered with PCA analysis (Maier et al., 1987; Achim et al., 1988; also cf. Mosher et al., 1992). One goal of this study was to use simulated data with known cortical sources to determine how well the PCA algorithm recover the cortical sources.

An alternative linear decomposition method could be used in this manner. The "independent component analysis" (ICA) (Makeig et al., 1996, 1997) provides a linear decomposition of data and has been applied to EEG and ERP. The ICA approach has been described in several places (Makeig et al., 1996, 1997; Jung et al., 2000a,b). As with PCA, the ICA attempts to discover a set of component weights that represent filters that linearly decompose a set of data. The ICA uses an "infomax" algorithm that attempts to minimize the common information among the temporal projections derived from single component weights and their accompanying activations, and maximize the information in each component. The output of the projected

activation for one component is statistically independent from the output of other components (Jung et al., 2000a), though the weights of one component are not necessarily orthogonal to other component weights.

The ICA approach may be applied to the source analysis problem. If ICA is applied to multichannel EEG recording, the component weights produced by the ICA approach are a set of topographical scalp maps similar to the PCA eigenvectors (Jung et al., 2001a,b). Thus, the ICA component weights could be used in equivalent current source analysis to model the dipoles that generated scalp-recorded EEG activity. A recent use of ICA has applied it to single trial EEG data, extracted components, and estimated equivalent current dipoles from the resulting component weights (DeLorme et al., 2002; Jung et al., 2000b, 2001a). Either approach (ICA, PCA) can be used with "spatial component analysis" to describe the scalp topography of an ERP component, and temporal activations of the component(s) describe the temporal morphology of the ERP component.

Several authors using and describing the ICA approach have been critical of the use of PCA for uncovering cortical sources in EEG and ERP data (Jung et al., 2000a; Makeig et al., 1997, 1999). For example, one criticism is that if the sources of neural activity are temporally sparse and the resulting EEG data decidedly non-normal, the PCA decomposition might result in single components with linear combinations of the underlying sources rather than separating sources into distinct components. Another criticism of the PCA technique is that neurophysiological models do not necessarily imply orthogonality of cortical sources, and the possibility of non-orthognal component weights is preferable for ERP data. Therefore, ICA might have an advantage in discriminating between brain sources whose spatial projection to the recording EEG electrodes are non-orthogonal (Makeig et al., 1999). The ICA technique has some assumptions that may not be met in ERP components. The ICA technique assumes that the temporal activity making up the underlying sources are independent (Jung et al., 2000b). Therefore, dipole sources with a consistent temporal overlap could not be successfully distinguished by the ICA component weights. Whether the ICA or the PCA approach is preferable for a cortical source analysis does not seem resolvable by theoretical arguments. Some studies have compared the two methods with empirical data (e.g., Makeig et al., 1997, 1999) and prefer the ICA results. One goal of the current study was to compare the results from ICA analysis and PCA analysis for uncovering dipole sources in simulated data with known cortical or cerebral sources.

There were three main procedures used in the study. First, I simulated ERP data using cerebral sources in five different datasets. The sources came from brain areas that were reasonable examples of ERP component sources. The datasets differed in the amount of spatial overlap in the sources (orthogonality of dipole sources) and amount of temporal overlap in the activity of the sources (temporal independence of cortical source activity). These variables could conceivably affect how well the PCA and ICA techniques worked. Second, spatial component analysis (PCA and ICA) was applied to the simulated ERP data to recover the topographical and temporal aspects of the ERP components (DeLorme et al., 2002; Jung et al., 2001b; Richards, 2003, 2004). The component weights were used with topographical maps to see if the weights were similar to the topographical distributions in the source ERP (following, e.g., Makeig et al., 1996, 1997 for ICA, and Spencer et al., 1999 for PCA). The time course of the ERP components was analyzed with the "principal component scores" for PCA, and the "activations" for ICA. This consists of a score for the component along each point in the temporal sequence of the ERP segments, the "temporal activation" of the component (following, Makeig et al., 1996, 1997). Third, cortical source analysis (equivalent current dipole analysis; e.g., Scherg, 1990, 1992; Scherg and Picton, 1991; Huizenga and Molenaar, 1994) was used to recover the sources that generated the data. The overall approach I followed was similar to that done by DeLorme et al. (2002) and Jung et al. (2001b) with ICA, who used spatial component analysis followed by equivalent current dipole analysis of the component weights.

2. Method

2.1. Cortical sources, EEG segments and the forward solution

Seventeen locations in the cortex and one location in the hippocampus were chosen as dipole sources.

Table 1 has the anatomical names of the locations. The sources were chosen based on source analysis studies, neuroimaging work, neurophysiological data, and ERP work. Each source was located via the standardized "Talairach" maps (Talairach and Tournoux, 1988; see Table 1). A structural MR recording was made for one individual and scalp/skull landmarks were identified and measured. The source was then identified according to the mm coordinates of that individual (Table 1).

The EMSE computer program was used to generate EEG segments using the forward solution. Each segment consisted of 400 ms of data sampled at 500 Hz, i.e., 200 samples. The EEG segments were generated for a 128-channel EGI sensor system (Electrical Geodesics, Eugene, OR; Tucker, 1993; Tucker et al., 1994) using the electrode placement file for the individual. The temporal course of the source activity was the same for each ERP segment, and consisted of a inverse exponential increase and decrease over about 200 ms of the interval. The dipole magnitude was set to 1.0e−07 in each case. In addition, EEG noise was generated at 10% amplitude of the dipole (1.0e−08 amplitude; pseudo-random Gaussian signal added to each channel). In addition to the specific sources required by the simulations goals (next section), all EEG segments contained at least one dipole from the sources in Table 1 at 0.25e−07 amplitude and whose temporal onset varied randomly in each segment. The datasets were generated by choosing one of these random sources, one of the sources relevant to the simulations goal, and generating 160 trials (32,000 samples).

2.2. Five simulated datasets

Five datasets were simulated. Each dataset had four conditions. One condition always was a control trial that had only a randomly chosen dipole source. For two of the datasets, I chose sources from Table 1 that had little spatial overlap. Fig. 1 shows the topographical potential maps for the anterior cingulate, middle temporal, and extrastriate visual sources. These sources might reasonably occur in a cued fixed foreperiod reaction time task. This task is known to generate a contingent negative variation in EEG, the CNV (Fabiani et al., 2000; Walter et al., 1964) which could be modeled as having a cortical source located in the anterior cingulate cortex. The spatial cueing should result in an enhancement of the ERP occurring over occipital scalp leads, the P1 validity effect, which is caused by activity in extrastriate visual cortex (Hillyard et al., 1995; Martinez et al., 1999; Richards, 2003, 2004). Spatial overlap between two sources was

Table 1
Cortical sources for the experiments

No.	Anatomical location	Talairach coordinates			Brodmann area
		Coronal	Saggital	Axial	
1	Anterior cingulate	25	13	20	32
2	Extrastriate visual	−95	29	20	18
3	Middle temporal	−25	51	−15	21
4	Superior temporal sulcus (parallel dipole)	9	39	10	22
5	Fusiform gyrus	−70	33	−10	37
6	Striate visual (parallel dipole)	−80	19	0	17
7	Frontal eye fields	−7	20	51	6
8	Dorsolateral prefrontal	25	47	26	46
9	Hippocampus	−46	−18	−12	Hippocampus
10	Inferior temporal	−17	55	−27	21
11	Frontal pole	64	1	17	10
12	Sensorimotor eye fields	11	40	46	8
13	Medial cingulate	−15	11	42	31
14	Superior posterior cingulate (parallel dipole)	−41	11	36	31
15	Prefrontal	44	33	0	10
16	Primary auditory	−29	41	−22	20
17	Wernicke's area	−66	58	−11	38
18	Broca's area	15	29	74	47

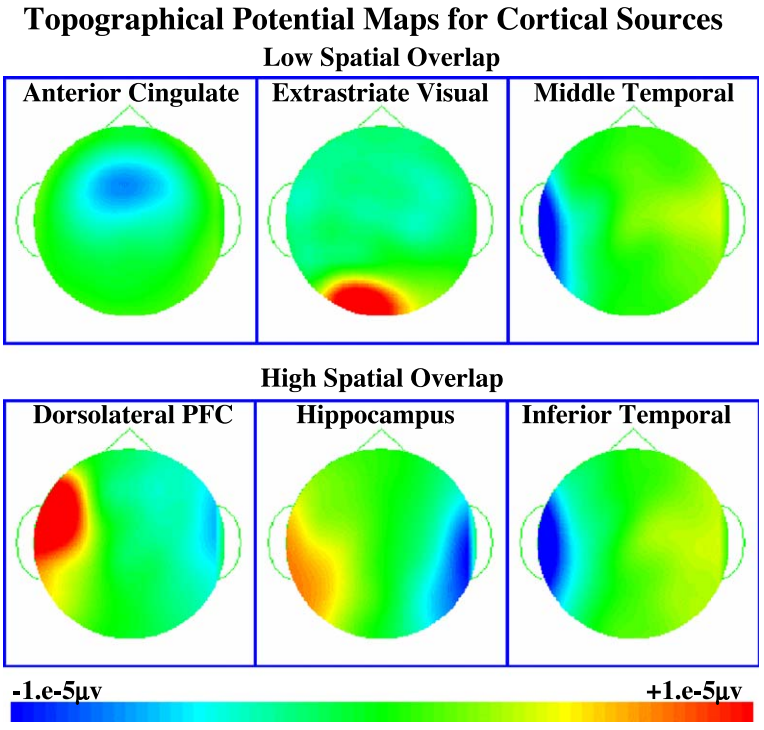

Fig. 1. Topographical potential maps for the low spatial overlap and the high spatial overlap cortical sources.

measured by computing the correlation between the 128 electrodes at the peak of the EEG. The correlation for these sources was relatively small (anterior cingulate and extrastriate visual, r=0.309; anterior cingulate and middle temporal, r=−0.168; extrastriate visual and middle temporal, r=0.021). The *Single Sources, No Overlap* dataset was generated with only one of these sources on each trial. Fig. 2 shows the spatiotemporal topographical potential map for the middle temporal trial. Because a trial was generated by a single source, there was no spatial and no temporal overlap from the sources in the EEG segments. The *Additive Sources, Temporal Overlap* dataset was generated so that sources were successively added to each trial. That is, one trial had only the anterior cingulate source, one trial had the anterior cingulate and extrastriate visual source, and one trial had all three sources. Fig. 2 shows a spatiotemporal topographical potential map for the trial with the three sources. The onset of the anterior cingulate source varied randomly, whereas the extrastriate visual and middle temporal sources had their peak occur at the same interval (about 200 ms).

Two of the datasets had sources with significant spatial overlap. Fig. 1 shows the topographical potential maps for the dorsolateral prefrontal, hippocampus, and inferior temporal sources. These sources might reasonably occur in an experiment evaluating working memory and long-term memory. The hippocampus and the inferior temporal cortex are known to be involved in long-term storage (Monk et al., 2000; Nelson, 1995). The dorsolateral prefrontal cortex is involved in working memory (Levy and Goldman-Rakic, 1999). The correlation of the peak EEG between the 128 electrodes was large (dorsolateral prefrontal and hippocampus, r=0.724; dorsolateral prefrontal and inferior temporal, r=−0.803; hippocampus and inferior temporal, r=−0.764). The *Single Sources, Spatial Overlap* dataset was generated with only one of these sources on each trial. The *Additive Sources, Temporal and Spatial Overlap* dataset was generated with the sources successively added to each trial. One trial had only the dorsolateral prefrontal source, one trial had the dorsolateral prefrontal and hippocampus sources, and one trial had all three sources. Fig. 2 shows a spatiotemporal topographical

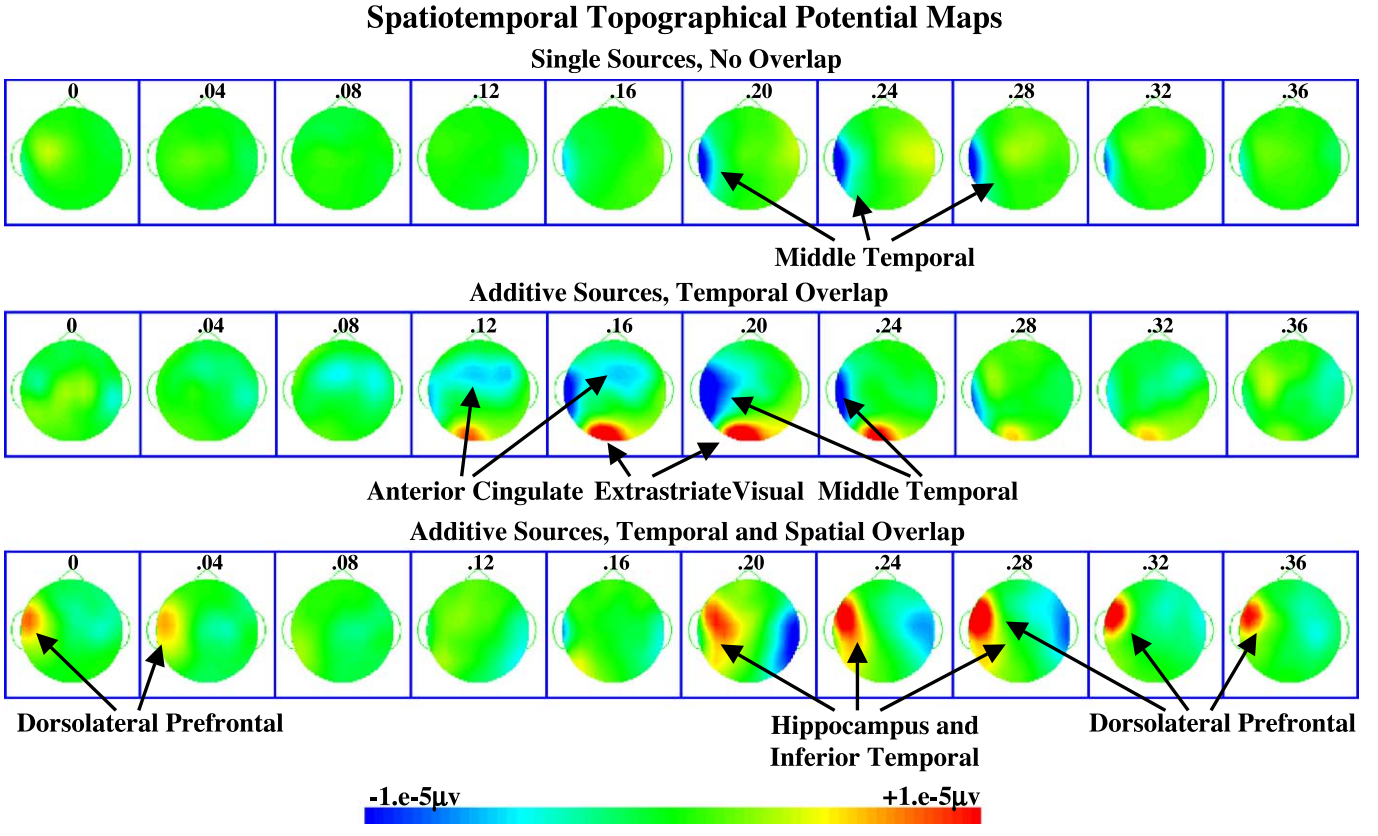

Fig. 2. Spatiotemporal topographical potential maps for three of the simulated datasets. The maps represent the EEG segment of a single 400 ms trial in 40 ms averages for the three displayed datasets.

potential map for the trial with the three sources. The dorsolateral prefrontal source had its temporal onset varied randomly, whereas the extrastriate visual and middle temporal sources always had their peak occur at the same interval.

The *Multiple Sources* dataset was generated with nine cortical sources underlying the EEG segments. One trial had the three sources from the low spatial overlap sources (Fig. 1), one trial had the sources from the high spatial overlap sources (Fig. 1), and one trial had three sources with mixed spatial overlap (fusiform gyrus and superior temporal sulcus, $r=-0.108$; fusiform gyrus and striate visual, $r=-0.219$; superior temporal sulcus and striate visual, $r=-0.816$). These latter three sources might reasonably be involved in a study of face processing (de Haan and Nelson, 1999). Each source in a trial had its starting point randomly chosen in the first 300 ms of the 400 ms sample interval, so that the sources were temporally overlapping in most of the trials.

2.3. Principal component analysis

The PCA was done following the procedures used by Richards (2003). The analysis was done on the "raw EEG" data, i.e., no ERP averages were studied. One advantage of this approach is that the activations may be viewed on single trials for single participants, and related to participant characteristics (i.e., age, gender) or single trial results (i.e., reaction time, error rate, memory performance). The PCA was done as a "spatial PCA" (Spencer et al., 1999). Fig. 3 shows how the EEG was arranged in a matrix. The variables for the analysis were the 128 electrode sites (columns of EEG Data Matrix in Fig. 3), and the observations were the time-sampled EEG data for the 128 channels (rows of EEG Data Matrix in Fig. 3). The data from the 160 trials were concatenated (Segment 1, Segment 2, . . . Segment 160 in rows of EEG Data Matrix in Fig. 3). This resulted in 4 trial types×40 trials per type×200 samples per trial=32,000 observations. For an ERP study, this might represent the data from a single individual (see DeLorme et al., 2002; Jung et al., 2001b for a similar approach with ICA). The PCA resulted in a set of 128 component loadings, with each component having a loading for the 128 electrode channels (Component Loading Matrix in Fig. 3). Because the PCA was done on the covariance matrix,

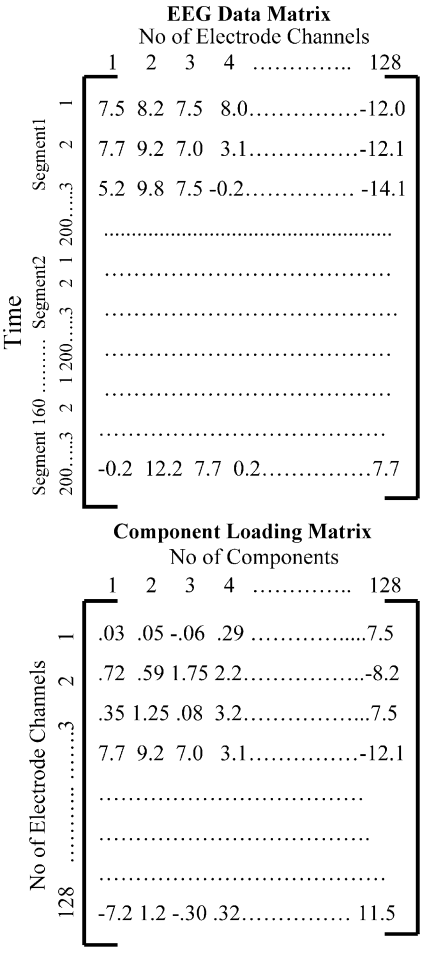

Fig. 3. The matrix of observations for the PCA and ICA analysis, for a "spatial PCA" (spatial ICA) component analysis, and the matrix of component loading weights.

the eigenvector weights represent the coefficients for computing the principal component scores from the raw data.

The resulting component weights (eigenvector values) were used to display in topographical plots the spatial organization of the components (Richards, 2003, 2004; Spencer et al., 1999). For example, the 128 weights corresponding to the electrode channels in the first column of the Component Loading Matrix in Fig. 3 would represent the weights being plotted in a topographical map for the first principal component. These plots represent topographically coordinated activity that is temporally concomitant in the ERP data but is independent of the temporal information and independent of the experimental factors. The

topographical maps consisted of a spherical spline interpolation (Perrin et al., 1989) shown in a radial projection (Perrin et al., 1987). For the topographical maps, the principal component weights were multiplied by the standard deviation of the original variables, and thus were displayed in μV units. This transformation was done so that the topographical maps from the PCA would be in the same units as those from the ICA, which intrinsically are in μV units.

The temporal information is lost in the component weights. Thus, the temporal morphology of the components was analyzed by examining the "component scores" for each component along each point in the temporal sequence of the ERP segments, the "temporal activation" of the component (Makeig et al., 1996, 1997). The activations were found by multiplying the 128 raw EEG data points at 2 ms samples in matrix multiplication with the 128 weights for a component, thus resulting in a single component activation score for each 2 ms sample. The matrix of activations is equivalent to the EEG Data Matrix multiplied by the Component Loading Matrix shown in Fig. 3. These activations may be shown trial-by-trial, averaged over several trials, or analyzed via factorial designs experimental factors.

2.4. Independent component analysis (ICA)

An independent component analysis (ICA) was done following the procedures outlined by Makeig, Sejnowski, and their associates (DeLorme et al., 2002; Jung et al., 2001b; Makeig et al., 1996, 1997; also see Reynolds and Richards, 2004; Richards, 2004). The ICA was done on the same data used for the PCA, i.e., raw EEG stacked from the 160 trials, 32,000 samples (EEG Data Matrix in Fig. 3). The variables for the analysis were the 128 electrode sites, leading to the estimation of 128 components (DeLorme et al., 2002; Jung et al., 2001b). Each ICA component had loadings analogous to the PCA technique, with each component having a loading for the 128 electrode channels (Component Loading Matrix in Fig. 3). The weights were calculated using the extended-ICA algorithm of Lee et al. (1999), with an initial learning rate of 0.003. The activations were calculated. Topographical maps and temporal activations were obtained in parallel to the PCA procedures.

The inverse of the resulting component weights was calculated. This matrix represents the scoring matrix against which the activations would be multiplied to restore the raw data, i.e., the matrix of ICA component activations would be equal to the EEG Data Matrix multiplied by the inverse of the Component Loading Matrix for the ICA analysis. This matrix is analogous to the eigenvector matrix computed in PCA. The ICA weights from this matrix were used display in topographical plots the spatial organization of the components (Makeig et al., 1996, 1997). These weights were in μV units so that the topographical maps from the PCA and ICA were in comparable units.

2.5. Cortical source analysis

The cortical source analysis used equivalent current dipole analysis. Component weights (PCA or ICA) were analyzed with equivalent current dipole analysis to determine the fit between the weights describing the component and scalp current generated by hypothetical dipoles (DeLorme et al., 2002; Jung et al., 2001b). Dipole source analysis hypothesizes a (a set of) dipole (s) that generates an electrical current on the scalp. This forward solution may be compared with the component weights, and the dipole location and magnitude is modified to minimize the difference between the generated current map and the component weights. I used single- and multiple-dipole sources. I accepted a single-dipole source model if the model explained at least 95% of the variance. Otherwise, a second dipole was added to the analysis. There were some models that required three-dipole sources to explain greater than 95% of the variance in the component weights. For the single-dipole models, I first estimated model fit for a dipole with fixed locations but whose moments were estimated, and then a model with estimated locations and moments. Multiple-dipole models had only fixed locations and free moments.

2.6. Computer programs

The MR Viewer (Signal Source Imaging) was used to identify the Talairach locations and the mm

locations for the individual and to view the MRIs. The EMSE computer program from the same company was used to simulate the ERP segments, display the topographical maps, and do the source analysis (BESA is an alternative program for such analyses). I used SAS programs to combine the forward solution ERP segments according to the five simulated datasets. The programs generated 1 trial for each condition and were run 40 times to acquire 40 trials per condition. The SAS Proc Principal was used for the PCA. The SAS programs are available from the author. The extended-ICA algorithm was originally programmed in Matlab by Scott Makeig and others, and I used the publicly available program done in C++ from the Matlab versions by Sigurd Enghoff (March, 2000; see http://www.cnl.salk.edu/~enghoff/).

3. Results

3.1. Components analysis and source analysis

3.1.1. Single Sources, No Overlap

This dataset was generated with only a single source on each trial, so there was no temporal or spatial overlap from the sources in the EEG segments. Fig. 2 shows a spatiotemporal topographical potential map for a middle temporal trial. The eigenvector weights from the PCA are shown in a topographical display in Fig. 4 for the first 10 components of each analysis. The equivalent current dipole modeling was applied to the first three components of the PCA. A single-dipole model for the first component accounted for 92% of the variance when the location was fixed at the middle temporal source location, and 97% of the variance with location estimated. This model placed the dipole at [−15, 44, −14], which was about 7 mm away from the middle temporal source. A single-dipole model with a fixed location at the extrastriate visual source for the second PCA accounted for 97% of the variance, and estimating the dipole location resulted in a dipole less than 2 mm from the extrastriate source. A single-dipole model at the anterior cingulate explained only 83% of the variance in the third PCA, whereas a model with a sources at this location and at the extrastriate visual location accounted for 97% of the component weights variance. These results imply that the first three PCA components contain the three sources for this simulated dataset.

The equivalent current dipole model was applied to the ICA components shown in Fig. 4. It appears in this figure that the sources were reflected in several ICA components. Models with a fixed dipole in the middle temporal source accounted for 95%, 98%, 96%, 92%, and 96% of the ICA components numbered 2, 3, 5, 6, and 9, respectively. Estimating the location of the dipole resulted in dipole locations close to the middle temporal source, e.g., [−22, 49, −12] for component 2, which was 3 mm away from the middle temporal source. Single-dipole models that were fixed at the extrastriate source or estimated locations for ICA components 1, 7, 8, and 9 resulted in models that accounted for 94–98% of the variance in the component weights. The fourth ICA component was modeled well by a fixed dipole at the anterior cingulate location (98%), and an estimated location for this component was [23, 15, 17], about 3 mm away from the anterior cingulate source. These results affirm the impression that several ICA components consisted of the sources used to generate the EEG segments.

The patterns of activation of the components were examined. Fig. 5 shows the activation patterns for the first three PCA components on the trials in which the extrastriate visual source or the middle temporal source was active. The top left panel shows that the activation of the second PCA occurred in the same time interval that the extrastriate source was active in generating the EEG segment. The top right panel shows similar activation for the first PCA and the middle temporal source. These activation patterns confirm the visual impression from the topographical maps and the equivalent current source analysis that the first PCA reflected the middle temporal source and the second PCA reflected the extrastriate visual source.

The activation patterns for the ICA analysis were more complex than those of the PCA analysis. Fig. 5 shows the activation patterns for several ICA components in which the extrastriate visual source or the middle temporal source was active. Considering the first two ICA components (middle panels), there was a consistency between the activation patterns of the ICA components, the visual impression from the topographical maps, and the equivalent current source

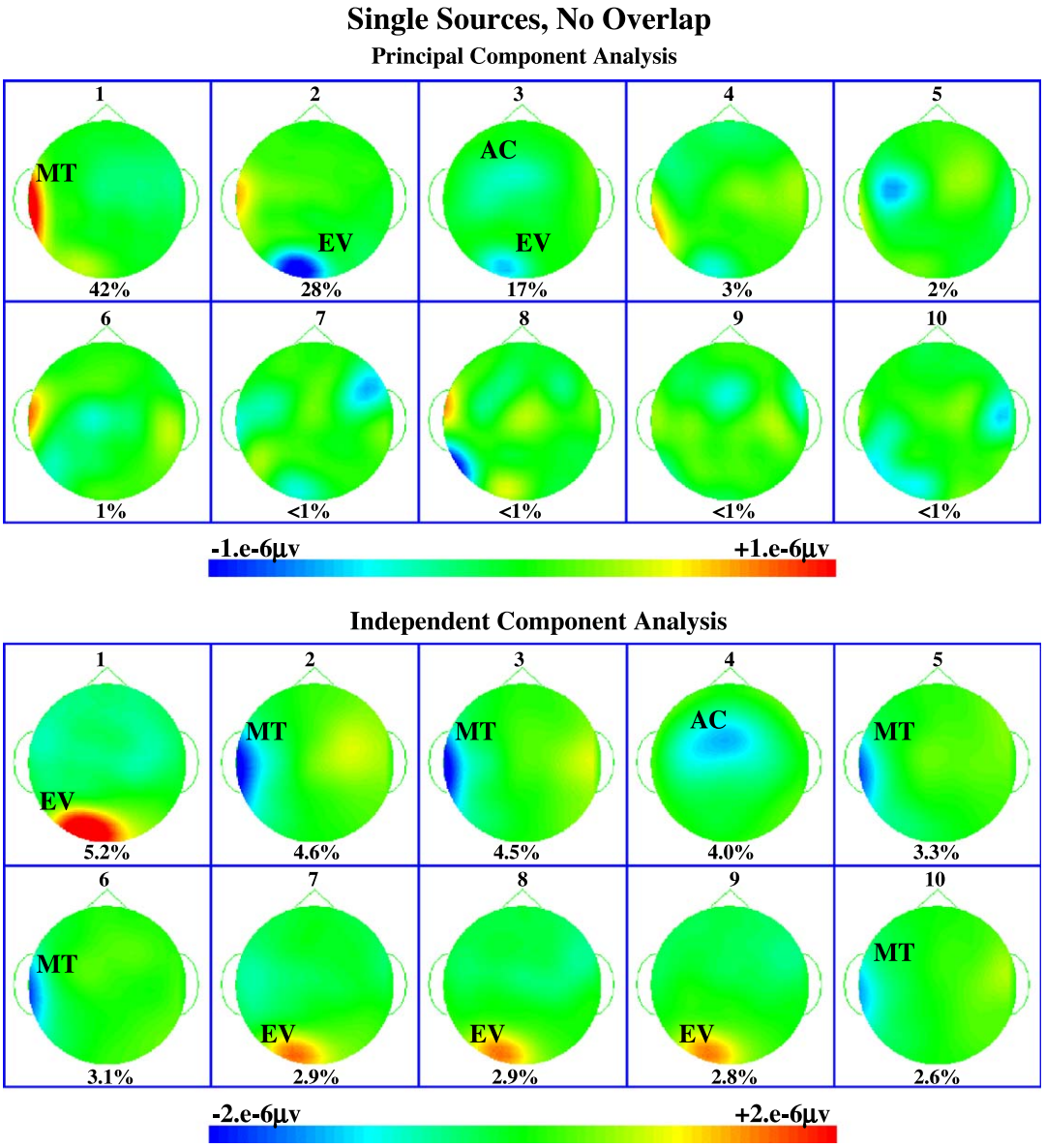

Fig. 4. Topographical maps of the eigenvector weights for the PCA analysis and the ICA component weights (inverse of weight*sphere matrix) for the *Single Sources, No Overlap* dataset. The percentages for the PCA components are the percent variance accounted for by this principal component, and the percentages for the ICA components are the relative variance from the projected data for this component. The ICA analysis results in μV units for this matrix, and the PCA eigenvector weights were multiplied by the standard deviation of each variable for display in μV units. The labels on the maps represent the equivalent current dipole sources for that component (EV: extrastriate visual; MT: middle temporal; AC: anterior cingulate).

analyses. However, the bottom panels show the activation patterns for the other ICA components that reflected the extrastriate visual or middle temporal course. The ICA components 1, 7, 8, and 9 showed significant activity on the extrastriate visual source trials (Fig. 5, lower left panel). This is consistent with the topographical maps (Fig. 4) and the equivalent current dipole analysis. One should note the different

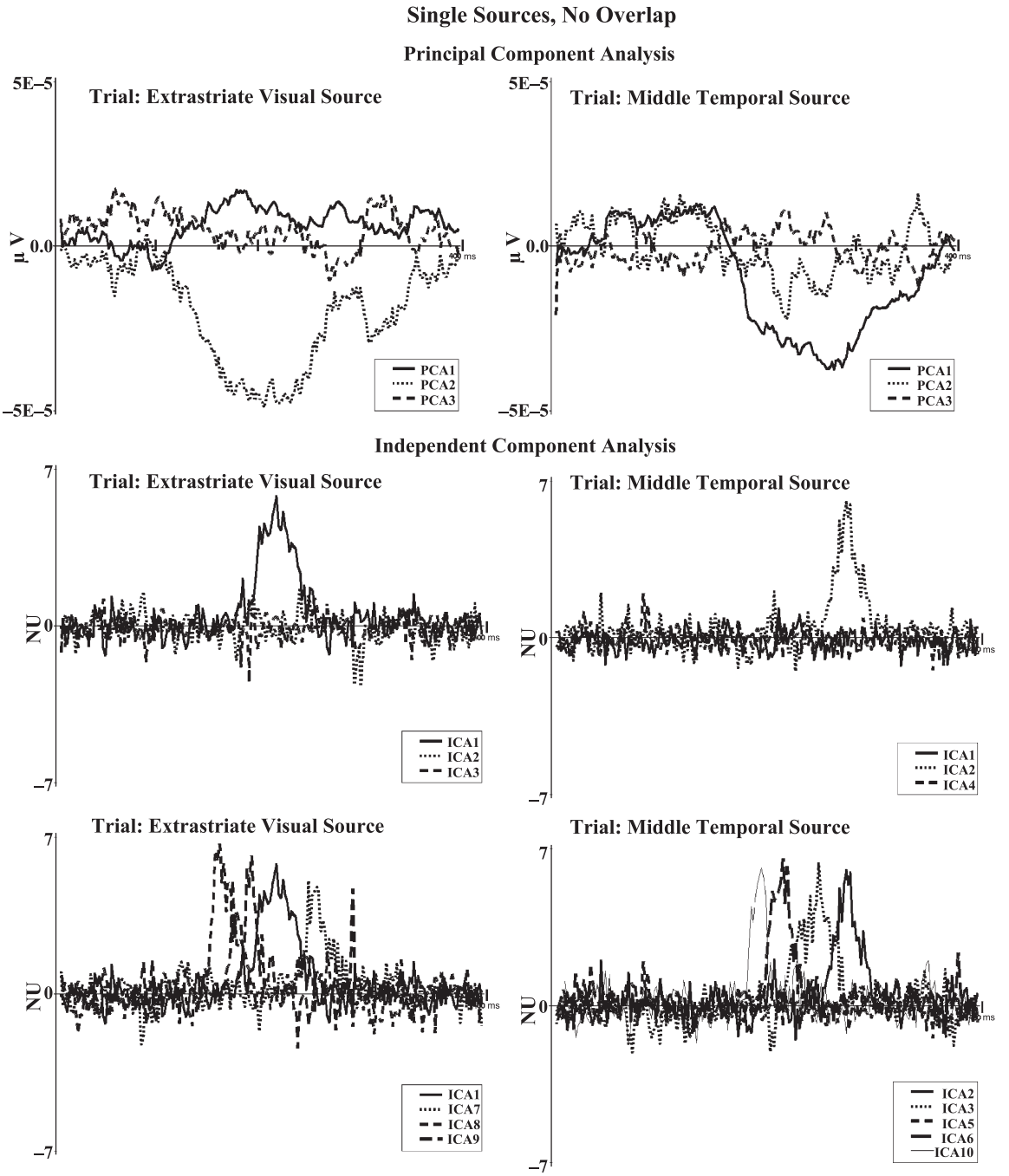

Fig. 5. Temporal activations (component scores over time) from PCA and ICA analyses for the *Single Sources, No Overlap* dataset, separately for the extrastriate visual source trials and the middle temporal source trials.

temporal course of activation for these components. The activations for the extrastriate visual source trials showed a temporal activation on each of the trials that was consistent with the mean activation time course. Since the temporal activity of the source generating the EEG segment was the same in each case, this suggests that the different components focused in on a different time segment of the source activity. This pattern was true for the multiple ICA components representing the middle temporal source (ICA components 2, 3, 5, 6, 10; Fig. 4 and bottom right panel of Fig. 5).

3.1.2. Single Sources, Temporal Overlap

This dataset was generated with sources that were successively added to the four trials and whose temporal activations overlapped in the EEG segment. These sources had little spatial overlap (Fig. 1). Fig. 2 shows a spatiotemporal topographical potential map for the trial that had the anterior cingulate, extrastriate visual, and middle temporal sources. The eigenvector weights for the first five PCA components are shown in a topographical display in Fig. 6. Only the first two PCA components were modeled well with the sources that were used to generate the dataset. The equivalent current dipole modeling resulted in two-dipole models. Single-dipole models with either fixed dipole locations or estimated dipole locations explained from 70% to 85% of the variance for the first component, and 67% to 87% of the variance in the second component. A two-dipole model with dipoles at the extrastriate visual and the middle temporal sources accounted for 95% of the variance for the first PCA component. A model with dipoles at the middle temporal and anterior cingulate sources accounted for 96% of the variance for the second PCA component. No other components were suitably modeled with single- or two-dipole models. The temporal activations for the first two components are shown in Fig. 6. The activation for the first PCA was largest on the trial when the extrastriate visual source and the middle temporal sources were active (right-hand figure). The second component showed a significant activation only when both the middle temporal and anterior cingulate sources were active (cf. right and left panels).

The equivalent current dipole model was applied to the ICA components shown in Fig. 6. Two-dipole models were necessary for the first four ICA components shown in Fig. 6. For the first two ICA components, the models required dipoles located at the extrastriate visual and middle temporal sources (98% and 96% variance accounted for). For the third and fourth ICA components, the models required dipoles located at the anterior cingulate and extrasriate visual sources (96% and 96% variance accounted for). The fifth ICA component was successfully modeled with a single-dipole source located at the anterior cingulate. A model with a fixed dipole source at the anterior cingulate accounted for 96% of the variance in the weights. Estimating the dipole locations resulted in a location at [25, 11, 13], which was 5 mm from the anterior cingulate source. The activation patterns for the first two components are shown in Fig. 6. Both components show a higher level of activation when both the extrastriate visual and the middle temporal sources were active (lower right panel). As with the single-source models (Fig. 5), the peak activation was slightly different for these multiple source components (Fig. 6, bottom right panel). I also examined several other ICA components not shown in Fig. 6. The three sources for this simulated dataset occurred in the same patterns as found in these first five components, i.e., one-dipole model for the anterior cingulate, two-dipole models for the middle temporal and extrastriate visual, and two-dipole models for the extrastriate visual and anterior cingulate.

3.1.3. Single and Additive Sources, Spatial Overlap and Temporal/Spatial Overlap

These datasets were generated with sources that had spatial overlap (Fig. 1), i.e., relatively large correlations between peak EEG amplitude at the electrodes. The *Single Source, Spatial Overlap* dataset had sources placed in separate trials, whereas the *Additive Sources, Temporal and Spatial Overlap* dataset had sources that were successively added to the four trials and whose temporal activations overlapped in the EEG segment. Fig. 2 shows a spatiotemporal topographical potential map for the trial that had the dorsolateral prefrontal, hippocampus, and inferior temporal sources. The eigenvector weights for the *Single Source, Spatial Overlap* dataset are shown in Fig. 7 only for the first PCA. The

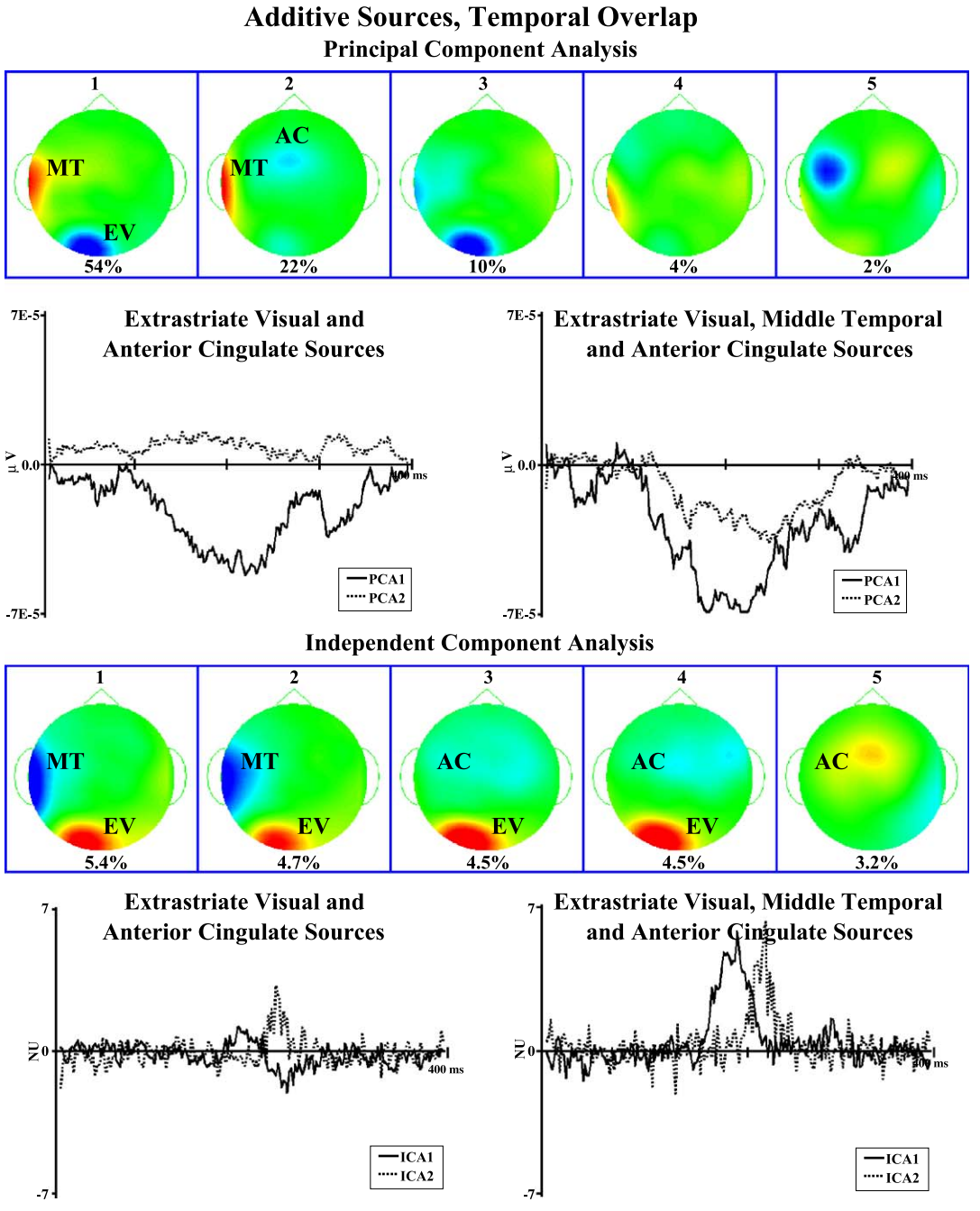

Fig. 6. First five ICA and PCA components for the *Additive Sources, Temporal Overlap* dataset. The color scale, percentages, units, and source labels for the components are the same as in Fig. 4.

equivalent current dipole modeling of the PCA components was done well only in the first component. The best fits for models with a single dipole at the dorsolateral prefrontal, hippocampus, or inferior temporal source, accounted for only 86% of the variance in the component weights. All three possible

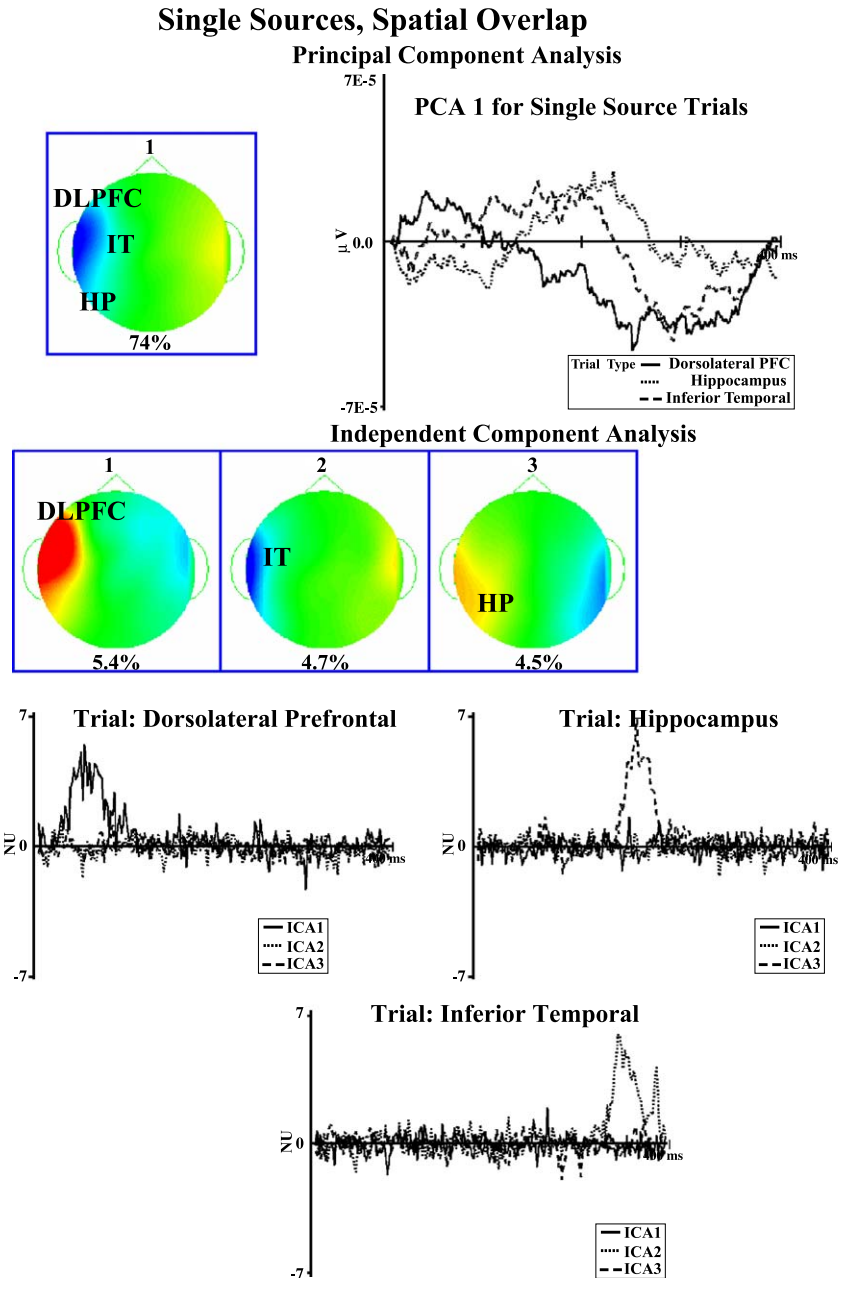

Fig. 7. First PCA components and first three ICA components for the *Single Sources, Spatial Overlap* dataset. The color scale, percentages, and units for the components are the same as in Fig. 3. The labels on the maps represent the equivalent current dipole sources for that component (DLPFC: dorsolateral prefrontal; IT: inferior temporal; HP: hippocampus).

two-dipole models worked well, accounting for 96% (dorsolateral prefrontal and hippocampus), 97% (dorsolateral prefrontal and inferior temporal), and 97% (hippocampus and inferior temporal) of the variance. A three-dipole model accounted for greater than 99% of the variance. Thus, although the two-dipole models worked well, there was a 2–3% increase with a three-dipole model.

The ICA resulted in components that had successful single-dipole models. Fig. 7 shows the topographical maps for the first three ICA components. A fixed location model with a single dipole at the dorsolateral frontal source location accounted for 98% of the variance. Estimating the location increased the accounted for variance to 99% and resulted in a location close to the dorsolateral prefrontal source, [20, 48, 20]. A single-dipole model with an inferior temporal location was a successful model for the

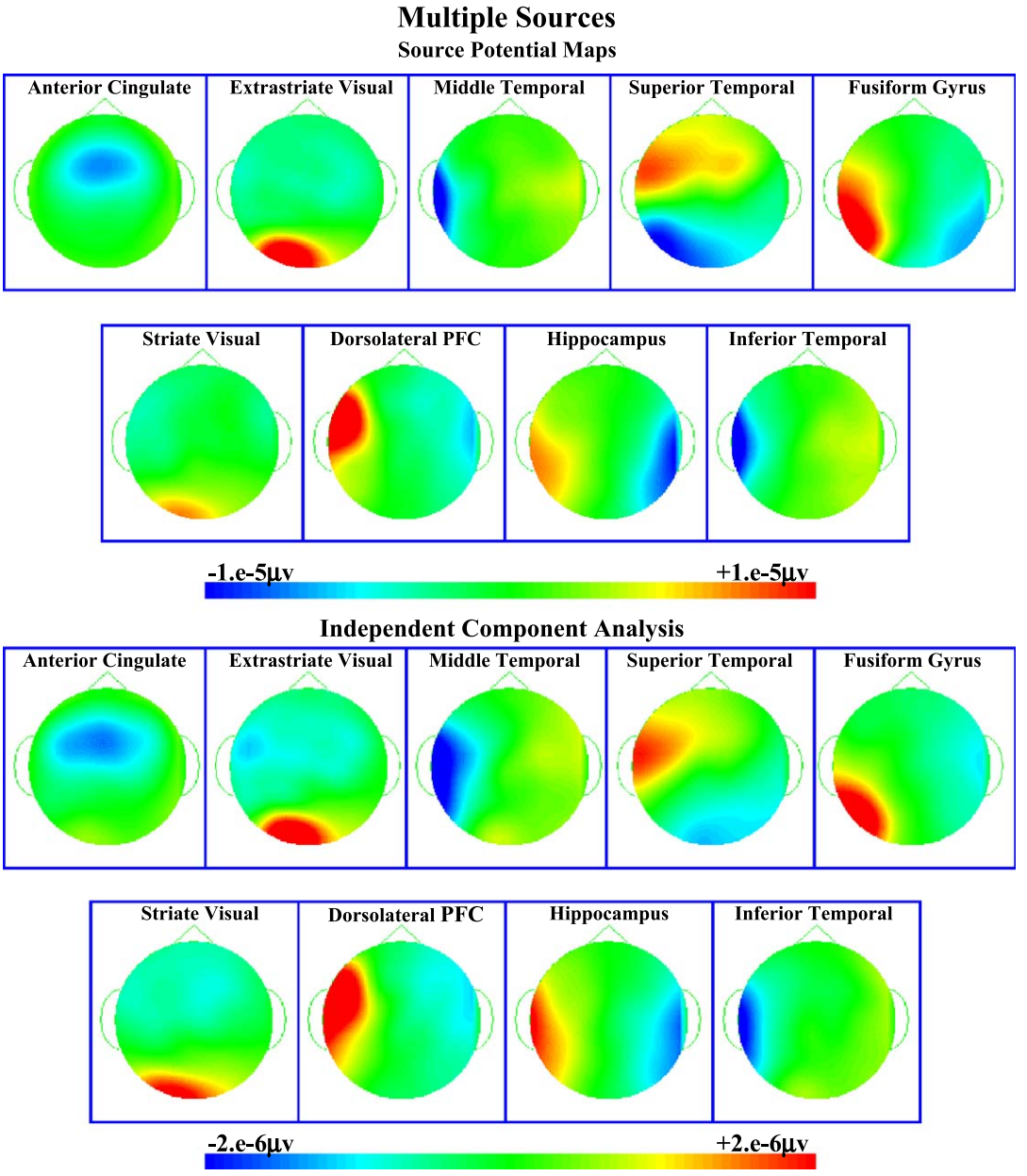

Fig. 8. The topographical potential maps and ICA components for the *Multiple Sources* dataset. The ICA components represent the first seven components of the ICA analysis, and components 12 (anterior cingulate) and 17 (inferior temporal). The labels on the ICA components represent the best-fitting single dipole model for that component.

second ICA component (97% and 98%) and a single-dipole model with a dipole at the hippocampus was a successful model for the third ICA component (98% and 99%). Fig. 7 shows the activation patterns for the first three ICA on the trials containing the single sources. The activations on these trials were consistent with the visual impression from the topographical sources and the equivalent current dipole analysis.

The *Additive Sources, Temporal and Spatial Overlap* dataset was evaluated. The results for the PCA components were nearly identical to the prior analysis; the first PCA component modeled by a three-dipole model. The analysis of the ICA components required single- and dual-dipole models. A single-dipole model with the dorsolateral prefrontal source resulted in models for ICA components 2, 3, 4, and 6 that accounted for between 94% and 99% of the variance in the component weights, and estimated locations were close to the dorsolateral prefrontal source. A two-dipole model with fixed locations was necessary for the first ICA component, consisting of a dorsolateral prefrontal and hippocampus source (98% variance). A two-dipole model was necessary for the tenth ICA component consisting of the dorsolateral prefrontal and inferior temporal sources (96% variance).

3.1.4. Multiple Sources

This dataset was generated with nine cerebral sources. One trial type had three sources with low spatial overlap, a second trial type had three sources with high spatial overlap, and one trial type had sources with mixed spatial overlap. The sources were temporally overlapping on most of the trials. The topographical maps of the sources are shown in the top part of Fig. 8. The equivalent current dipole analysis of the PCA components required two- or three-dipole models for successful models. For example, the first component was modeled with sources in the middle temporal and superior temporal sulcus (96%), the second component with anterior cingulate and extrastriate visual sources (97%), and the third component required a three-dipole model with anterior cingulate, striate visual, and inferior temporal sources (97%). All nine sources were required somewhere for the modeling of the first six PCA components. There did not seem to be an influence of temporal or spatial overlap that influenced which sources were needed on which components. For example, the hippocampus and dorsolateral prefrontal sources had temporal and spatial overlap and were needed on one component, but the superior temporal sulcus and middle temporal sources had no temporal overlap (occurred on different trials) and no spatial overlap ($r=-0.089$) but were necessary for the model of the first PCA component.

The topographical maps of the ICA components are shown in the lower half of Fig. 8, with labels on the ICA components reflecting the equivalent current dipole models for that component. The first seven ICA components were fit well with one-dipole models at a fixed location (95–97% variance accounted for) or at an estimated location (96–99%, and from 1 to 7 mm away from source). The anterior cingulate source successfully modeled the 12th ICA component (96%) and the inferior temporal source was the best fit on the 17th ICA component (94%). No two-dipole models were required for the fits of the ICA components in the *Multiple Sources* dataset.

4. Discussion

The goals of the study were to determine if the PCA or ICA analyses could recover dipole sources placed into simulated data and compare the two methods. The use of PCA outlined by Richards (2003), or ICA as outlined by Makeig, Sejnowski, and their associates (Jung et al., 2001a,b; Makeig et al., 1996, 1997; also see Richards, 2004), with analysis of the component with equivalent current dipole analysis, can recover sources placed into simulated data. This was true in the study under a variety of conditions that used cortical sources that resulted in ERP components that might be found in a typical cognitive psychophysiology or cognitive neuroscience experiment. This was true for cortical sources that had varying degrees of overlapping temporal sources and whose sources had non-orthogonal projections for the scalp surface. Both PCA and ICA recovered the generating sources in every dataset. There was no difference in the accuracy of localization for the recovered dipole sources between PCA and ICA, or in the amount of variance satisfactorily explained by dipole modeling with the generating sources. The analysis of the component loadings

recovered the dipole sources that were placed into the simulated data.

There were some differences in this study between ICA and PCA. In several cases, a PCA component required two sources in an equivalent current dipole model for sources that were explained with a single-source model for ICA. This was particularly noteworthy when the sources were spatially overlapping, i.e., showed non-orthogonal projections to the scalp electrodes. In this case a high degree of overlap produced a single PCA component that required three-dipole sources to successfully model the data. The ICA procedure resulted in single-dipole model for components with a high degree of spatial overlap (Figs. 7 and 8). The simulated dataset with nine cerebral sources favored the ICA approach. All PCA components required dual-dipole models to explain the component loading variance, whereas the ICA components were satisfactorily explained with single-source models. This is particularly interesting for the ICA method, since the dataset with multiple sources contained sources that were generally temporally overlapping but who had random onsets. Thus, the lack of a consistent temporal activation pattern between sources resulted in single-source models even though temporal overlap occurred.

Another difference between the two methods was that for PCA only the first few components had information regarding the sources that were used to generate the data. The ICA had ERP component sources that occurred in multiple single-source components (Fig. 4), multiple dual-source components (Fig. 6), or multiple single-source and dual-source components (Fig. 6). This characteristic of the ICA components is likely due to the assumption that underlying sources have different and non-overlapping temporal activation patterns. The ICA algorithm resulted in similar spatial components with temporal activations that were of shorter duration than the underlying source duration (Figs. 5 and 6). The underlying source in each case lasted for about 100 ms, whereas activations of the ICA components lasted only about 20–30 ms. This could be seen as an advantage for the increased specificity of the ICA algorithm. However, if one considered the source activation pattern to be related to a cognitive process that generated the longer-lasting activation of the underlying source, then the PCA component activation covering the entire time interval of the generating source (Figs. 5 and 6) might be considered more beneficial. The phenomenon of multiple components with similar spatial topography appears in real EEG data (Jung et al., 2001a,b).

Many of the results in this study were consistent with the underlying assumptions of the methods. For example, under conditions of both temporal and spatial independence in the topography and activation of the generating sources, both methods predominantly resulted in components that could be adequately modeled with single-dipole models. There are some conditions for PCA, therefore, in which a single dipole (location and moment parameters) may be derived from single components for segmented EEG data (Maier et al., 1987; Achim et al., 1988; also cf. Mosher et al., 1992). Temporal correlation between generating sources has long been known to affect temporal PCA (Dien, 1998; Wood and McCarthy, 1984). Similarly, the ICA method assumes independence between the temporal activations of the underlying sources (Jung et al., 2000b, 2001a,b). The temporal overlap introduced into the simulated dataset resulted in PCA and ICA components requiring multiple-dipole models. The PCA was more sensitive to the temporal independence assumption, since the ICA results contained components successfully modeled by single-dipole models for the source (anterior cingulate, dorsolateral prefrontal cortex) that had some trials in which no other sources were present. The spatial PCA was more sensitive to spatial overlap in the generating sources than was the ICA (Fig. 7). This might be expected since the separate components of PCA are defined to be orthogonal, whereas the component weights of ICA are not necessarily orthogonal. Apparently, the non-orthogonality of the generating sources is represented in PCA by forcing the representation of the sources on single components.

Some authors using and describing the ICA approach have been critical of the use of PCA for cortical source analysis in EEG and ERP data (Jung et al., 2000a; Makeig et al., 1997, 1999). Some of these arguments raised concerning PCA were reflected in the current study's analysis. However, the results of the present study do not support a totally pessimistic view of the PCA approach. Even in the most negative

case for PCA, when the generating components were spatially non-orthogonal, the equivalent current dipole analysis still recovered the generating sources. When the timing of the temporal activation of the cortical sources was randomly distributed through the test interval, the PCA method resulted in components that distinguished nine cerebral sources in the EEG data segments. The ICA results were more likely to result in components that could be explained with single-source dipole models. However, in those cases the dipole models for the PCA method resulted in dipoles that were accurately localized and which explained the same amount of variance in the component weights.

There are some problems with dipole source analysis as applied to EEG and ERP data that are not answered or addressed in this paper. For example, the well-known "inverse problem" in dipole source analysis occurs because an infinite number of dipole generator configurations may be used to generate a specific ERP topography. In actual EEG and ERP data, several overlapping sources may generate a specific set of ERP results and it is difficult to estimate these multiple cortical dipoles with these methods. The analyses in the current paper were confined primarily to models in which a single-dipole location was known, or which two- or three-dipole locations were known. This corresponds more closely to a hypothesis-testing framework for such analyses in which other information constrains the locations in which one would look for dipole sources. One conclusion from the current analysis is that such models may be difficult to estimate with ICA when there is a large amount of temporal overlap between the sources. This would be a great disadvantage for this approach with some late ERP components (e.g., N4, late slow waves, P3) which may have EEG characteristics generated by a number of cerebral sources that have such temporal overlap. It may be that some of these conclusions, and the use of dipole source analysis in general, will apply more closely to ERP components that are generated by a small number of discrete cerebral sources.

The current study provides support for both PCA and ICA techniques in the study of dipole sources of ERP components. The use of such simulated data suggests that under certain conditions both methods are equally useful, whereas extreme spatial and temporal overlap strain the PCA technique more than the ICA technique. A further beneficial step would be to compare these procedures with empirical data. This could be done by comparing the two procedures in their analysis of ERP data (e.g., Makeig et al., 1997, 1999). However, such comparisons would have to be based on internal characteristics of the modeling (e.g., variance accounted for) or the relation of the results to experimental variables. Another approach would be to compare such modeling when the sources of the ERP components are known from other methods (e.g., fMRI or PET). An example of such an approach is that used by Martinez et al. (1999). They did structural MRI, fMRI, and ERP analysis of a spatial cueing procedure and were able to establish the location (fMRI and dipole analysis of raw ERP) and timing (ERP) of the P1 validity effect, even to showing an early and late P1 effect occurring in different cortical areas. Though they did not use component approaches such as PCA or ICA, conceivably such a multi-measurement approach could be accompanied by component analysis to test the validity of this analysis for recovering from the ERP the cortical sources identified in the fMRI. Such empirical analyses would answer the additional qualification of cognitive neuroscience that other neuroimaging tools (e.g., fMRI, PET) give complementary information regarding these components.

Acknowledgments

This research was supported by grants from the National Institute of Child Health and Human Development, #R01-HD18942 and a Major Research Instrumentation Award, # BCS-9977198, from the National Science Foundation. I wish to acknowledge Mark Johnson, Gergely Csibra, and others at the Center for Cognitive and Brain Development, Birbeck College, University College London, for their comments and suggestions, support of this work, and for hosting me in London while I did this work.

References

Achim, A., Richer, F., Saint-Hilaire, J., 1988. Methods for separating temporally overlapping sources of neuroelectric data. Brain Topography 1, 22–28.

Chapman, R.M., McCrary, J.W., 1995. EP component identification and measurement by principal components analysis. Brain Language 27, 288–301.

de Haan, M., Nelson, C.A., 1999. Brain activity differentiates face and object processing in 6-month-old infants. Developmental Psychology 35, 1113–1121.

DeLorme, A., Makeig, S., Fabre-Thorpe, M., Sejnowski, T., 2002. From single-trial EEG to brain area dynamics. Neurocomputing 44–46, 1057–1064.

Dien, J., 1998. Addressing misallocation of variance in principal components analysis of evoked potentials. Brain Topography 11, 43–55.

Dien, J., 1999. Differential lateralization of trait anxiety and trait fearfulness: evoked potential correlates. Personality and Individual Differences 26, 333–356.

Dien, J., Tucker, D.M., Potts, G., Harty-Speiser, A., 1997. Localization of auditory evoked potentials related to selective intermodal attention. Journal of Cognitive Neuroscience 9, 799–823.

Donchin, E., Ritter, W., McCallum, W.C., 1978. Cognitive psychophysiology: the endogenous components of the ERP. In: Callaway, E., Tueting, P., Koslow, S.H. (Eds.), Brain Event-Related Potentials in Man. Academic Press, New York.

Fabiani, M., Gratton, G., Coles, M.G.H., 2000. Event-related brain potentials: methods, theory, and applications. In: Cacioppo, J.T., Tassinary, L.G., Berntson, G.G. (Eds.), Handbook of Psychophysiology. Cambridge, New York, pp. 53–84.

Hillyard, S.A., Mangun, G.R., Woldroff, M.G., Luck, S.J., 1995. Neural systems mediating selective attention. In: Gazzaniga, M.S. (Ed.), Cognitive Neurosciences. MIT, Cambridge, MA, pp. 665–682.

Huizenga, H.M., Molenaar, P.C.M., 1994. Estimating and testing the sources of evoked potentials in the brain. Multivariate Behavioral Research 29, 237–262.

Jung, T.-P., Makeig, S., Humphries, C., Lee, T.-W., McKeown, M.J., Iragui, V., Sejnowski, T.J., 2000a. Removing electroencephalographic artifacts by blind source separation. Psychophysiology 37, 163–178.

Jung, T.-P., Makeig, S., Lee, T.-W., McKeown, M.J., Brown, G., Bell, A.J., Sejnowski, T.J., 2000b. Independent component analysis of biomedical signals. The 2nd International Workshop on Independent Component Analysis and Source Separation, pp. 633–644.

Jung, T.P., Makeig, S., McKeown, M.J., Bell, A.J., Lee, T.W., Sejnowski, T., 2001a. Imaging brain dynamics using independent component analysis. Proceedings of the IEEE 89, 1107–1122.

Jung, T.P., Makeig, S., Westerfield, M., Townsend, J., Courchesne, E., Sejnowski, T.J., 2001b. Analysis and visualization of single-trial event-related potentials. Human Brain Mapping 14, 166–185.

Lee, T.W., Girolami, M., Sejnowski, T.J., 1999. Independent component analysis using an extended infomax algorithm for mixed subgaussian and supergaussian sources. Neural Computing 11, 417–441.

Levy, R., Goldman-Rakic, P.S., 1999. Association of storage and processing functions in dorsolateral prefrontal cortex of the nonhuman primate. Journal of Neuroscience 19, 5149–5158.

Maier, J., Dagnelie, H., Spekreijse, H., van Dijk, B., 1987. Principal components analysis for source localization of VEPs in man. Vision Research 27, 165–177.

Makeig, S., Bell, A.H., Jung, T.P., Sejnowski, T.J., 1996. Independent component analysis of electroencephalographic data. Advances in Neural Information Processing Systems 8, 145–151.

Makeig, S., Jung, T.P., Bell, A.H., Ghahremani, D., Sejnowski, T.J., 1997. Blind separation of auditory event-related brain responses into independent components. Proceedings of the National Academy of Sciences 94, 10979–10984.

Makeig, S., Westerfield, M., Jung, T.P., Covington, J., Townsend, J., Sejnowski, T., Courchesne, E., 1999. Functionally independent components of the late positive event-related potential during visual spatial attention. Journal of Neuroscience 19, 2665–2680.

Martinez, A., Anllo-Vento, L., Sereno, M.I., Frank, L.R., Buxton, R.B., Dubowitz, D.J., Wong, E.C., Hinrichs, H., Heinze, H.J., Hillyard, S.A., 1999. Involvement of striate and extrastriate visual cortical areas in spatial attention. Nature Neuroscience 2, 364–369.

Monk, C.S., Zuang, J., Curtis, W.J., Ofenloch, I.T., Tottenham, N., Nelson, C.A., Hu, X., 2000. Human hippocampal activation in the delayed matching- and nonmatching-to-sample memory tasks: an event-related functional MRI approach. Behavioral Neuroscience 116, 716–721.

Mosher, J.C., Lewis, P.S., Leahy, R.M., 1992. Multiple dipole modeling and localization from spatio-temporal MEG data. IEEE Transactions on Biomedical Engineering 39, 541–557.

Nelson, C.A., 1995. The ontogeny of human memory: a cognitive neuroscience perspective. Developmental Psychology 31, 723–728.

Perrin, F., Bertrand, O., Pernier, J., 1987. Scalp current density mapping: value and estimation from brain data. IEEE Transactions on Biomedical Engineering 34, 283–288.

Perrin, F., Pernier, J., Bertrand, O., Echallier, J.F., 1989. Spherical splines for scalp potential and current density mapping. Electroencephalography and Clinical Neurophysiology 72, 184–187.

Reynolds, G.D., Richards, J.E., 2004. Familiarization and recognition memory in infancy: an ERP and cortical source localization study. Manuscript submitted for publication.

Richards, J.E., 2003. Cortical sources of event-related-potentials in the prosaccade and antisaccade task. Psychophysiology 40, 878–894.

Richards, J.E., 2004. Localizing cortical sources of event-related potentials in infants' covert orienting. Manuscript submitted for publication.

Scherg, M., 1990. Fundamentals of dipole source potential analysis. In: Grandon, F., Hoke, M., Romani, G.L. (Eds.), Auditory Evoked Magnetic Fields and Potentials, vol. 6. Karger, Basel, pp. 40–69.

Scherg, M., 1992. Functional imaging and localization of electromagnetic brain activity. Brain Topography 5, 103–111.

Scherg, M., Picton, T.W., 1991. Separation and identification of event-related potential components by brain electrical source analysis. In: Brunia, C.H.M., Mulder, G., Verbaten, M.N. (Eds.), Event-Related Brain Research. Elsevier Science Publishers, Amsterdam, pp. 24–37.

Spencer, K.M., Dien, J., Donchin, E., 1999. A componential analysis of the ERP elicited by novel events using a dense electrode array. Psychophysiology 36, 409–414.

Talairach, J., Tournoux, P., 1988. Co-planar Stereotaxic Atlas of the Human Brain. Thieme Medical Publishers, New York.

Tucker, D.M., 1993. Spatial sampling of head electrical fields: the geodesic sensor net. Electroencephalography and Clinical Neurophysiology 87, 154–163.

Tucker, D.M., Liotti, M., Potts, G.F., Russell, G.S., Posner, M.I., 1994. Spatiotemporal analysis of brain electrical fields. Human Brain Mapping 1, 134–152.

Walter, W.G., Cooper, R., Aldridge, V.J., McCallum, W.C., Winter, A.L., 1964. Contingent negative variation: an electrical sign of sensorimotor association and expectancy in the human brain. Nature 203, 380–384.

Wood, C.C., McCarthy, G., 1984. Principal component analysis of event-related potentials: simulation studies demonstrate misallocation of variance across components. Electroencephalography and Clinical Neurophysiology 59, 249–260.